

Landmark Detection and 3D Face Reconstruction for Caricature using a Nonlinear Parametric Model

Juyong Zhang, Hongrui Cai, Yudong Guo, Zhuang Peng

Abstract—Caricature is an artistic abstraction of the human face by distorting or exaggerating certain facial features, while still retains a likeness with the given face. Due to the large diversity of geometric and texture variations, automatic landmark detection and 3D face reconstruction for caricature is a challenging problem and has rarely been studied before. In this paper, we propose the first automatic method for this task by a novel 3D approach. To this end, we first build a dataset with various styles of 2D caricatures and their corresponding 3D shapes, and then build a parametric model on vertex based deformation space for 3D caricature face. Based on the constructed dataset and the nonlinear parametric model, we propose a neural network based method to regress the 3D face shape and orientation from the input 2D caricature image. Ablation studies and comparison with baseline methods demonstrate the effectiveness of our algorithm design, and extensive experimental results demonstrate that our method works well for various caricatures. Our constructed dataset, source code and trained model are available at <https://github.com/Juyong/CaricatureFace>.

Index Terms—Landmark Detection, 3D Face Reconstruction, Caricatures, Nonlinear Representation

I. INTRODUCTION

As a vivid artistic form that represents human faces in abstract and exaggerated ways, caricature is mainly used to express satire and humor for political or social incidents. It also has many applications in our daily life, including advertisements, electronic games, and so on. Since Brennan developed the first caricature generator in 1985 [1], the studies of caricatures have mainly focused on some specific tasks, such as caricature generation [2], [3], [4], [5], caricature recognition [6], [7], [8], and caricature reconstruction [9], [10], [11], [12]. Most of these tasks need facial landmarks to help to preprocess the caricatures. As a fundamental process for various caricature processing tasks, automatic facial landmark detection can greatly improve the efficiency and accuracy of other caricature processing tasks. As there is no automatic landmark detection method for caricature, all the present related works rely on manually labeling landmarks, which is tedious and time-consuming. Meanwhile, the reconstructed 3D model of caricature can be used for many applications, such as face animation, face editing and 3D printing, which need 3D geometry information.

Compared with other tasks like 3D caricature modeling and caricature recognition, there is little research on automatic

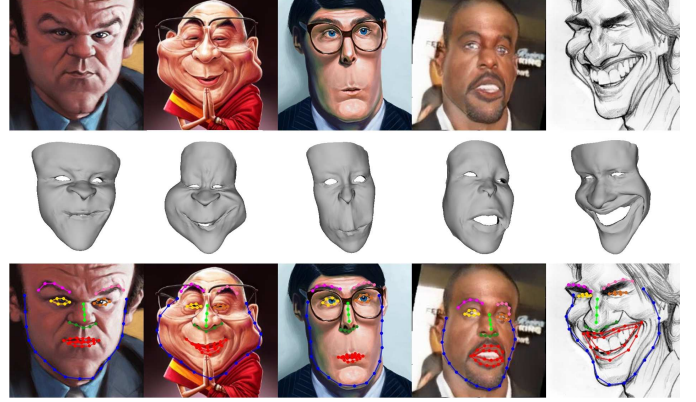


Fig. 1. Some examples of automatic landmark detection and 3D reconstruction on test set. Given a single caricature image (first row), our algorithm generates its 3D model with orientation (second row) and corresponding 68 landmarks (third row).

landmark detection for caricatures. As far as we know, one related work is proposed by Sadimon and Haron [13], which adopted the neural network to predict a facial caricature configuration. However, it can not process a single 2D caricature without its original facial image because the training dataset is constructed by image pairs- one normal facial image and its corresponding caricature image. Besides, their training and testing caricatures are all from exactly one artist, and thus the trained model can not be adapted to other caricatures with different art styles. There exist two main reasons to explain the difficulty of facial landmark detection for caricature. One reason is that caricatures have abstract and exaggerate patterns, and another is that caricatures have large representation varieties among different artists. As pointed out in [14], compared with landmark detection on normal facial images, it is much more challenging on landmark detection for caricatures.

In comparison to normal facial images, caricatures have two fundamental attributes- exaggeration and variety, and thus approaches for standard landmark detection can not be directly applied to solve this problem. One straightforward way is to regress the 2D landmarks' coordinates of caricature directly. However, 2D landmarks are controlled by facial shape and expression, facial orientation, and artistic style, which makes it a challenging problem to detect 2D landmarks. In order to alleviate the problem difficulty, we propose to decouple these factors. By regressing the 3D face model of caricature and face orientation, 2D landmarks can be recovered by projecting the 3D landmarks with the orientation.

Therefore, it is quite essential to propose a method to

J. Zhang, Y. Guo and Z. Peng are with School of Mathematical Sciences, University of Science and Technology of China.

H. Cai is with School of Data Science, University of Science and Technology of China.

represent the 3D face model of caricature. In 3D face reconstruction, parametric models, such as 3D Morphable Model (3DMM) [15], are usually used to represent 3D face shapes. However, such models are designed to represent normal face shapes and do not work well for caricature faces due to their limited capability of extrapolation [12]. In this paper, to solve this challenging problem, we specifically design a parametric model for 3D caricature faces, and propose a method for landmark detection and 3D reconstruction of caricature based on this model.

To this end, we manually label landmarks of about 6K caricature images with different styles. We further automatically generate nearly 2K caricatures with labeled landmarks from standard facial images via the method described in [4]. Based on the labeled landmarks, we recover the corresponding 3D caricature shape and orientations using an optimization method. With the large scale training dataset, we propose a novel convolutional neural network based method to regress the 3D caricature shape and orientation from the input 2D caricature. To well represent the 3D exaggerated face, we propose to regress its deformation representation rather than the Euclidean coordinates, which helps to improve the landmark detection and 3D reconstruction ability. In summary, the main contributions of this paper include the following aspects:

- To the best of our knowledge, this is the first work for automatic landmark detection and 3D face reconstruction for general caricatures.
- Rather than directly regress the 2D landmarks, we regress the 3D caricature shape and orientation from input 2D caricature image. 3D caricature shape is represented by a nonlinear parametric model learned from our constructed 3D caricature dataset.
- Comparisons with baseline methods and ablation studies demonstrate the effectiveness of each module of our proposed method. Extensive qualitative and quantitative experiments demonstrate that our method can automatically produce high accuracy results of 2D landmark detection and 3D shape reconstruction for caricature.

II. RELATED WORK

This section briefly reviews some works that related to this paper, with a special focus on face alignment and 3D face reconstruction for normal facial images, and face alignment and 3D face reconstruction for caricatures.

Face Alignment. Face alignment and landmark detection for normal facial images have achieved great success in the last few years with the power of convolution neural networks. Kazemi and Sullivan [17] used an Ensemble of Regression Trees to estimate the facial landmark positions, and their method has been integrated into Dlib library [18], a modern C++ toolkit containing some machine learning algorithms. Wu *et al.* [19] proposed *vanilla* CNN, which is naturally hierarchical and requires no auxiliary labels beyond landmarks. Kowalski *et al.* [20] developed Deep Alignment Network (DAN), a robust deep neural network architecture that consists of multiple stages. By adopting a coarse-to-fine Ensemble of Regression Trees, Valle *et al.* [21] proposed a real-time

facial landmark regression algorithm. Liu *et al.* [22] noticed that the semantic ambiguity degrades the detection performance and addressed this issue by latent variable optimization methods. Dong *et al.* [23] presented an unsupervised approach to improving facial landmark detectors, and Honari *et al.* [24] showed a new architecture and training procedure for semi-supervised landmark localization. To solve the occlusion problem, Zhu *et al.* [25] developed an occlusion-adaptive deep network, which contains a geometry-aware module, a distillation module, and a low-rank learning module. Merget *et al.* [26] proposed a novel network architecture that has an implicit kernel convolution between a local-context subnet and a global-context subnet composed of dilated convolutions.

3D Face Reconstruction from A Single Image. 3D face reconstruction from a single image is to recover 3D facial geometry from a given facial image, which has applications like face recognition [27], [28], face alignment [29], [30] and expression transfer [31], [32]. Since Blanz and Vetter proposed a 3D Morphable Model (3DMM) in 1999 [15], model-based methods have become popular in solving problems of 3D face reconstruction. Earlier, a large number of model-based algorithms considered some significant facial parts between 2D images and 3D templates, such as facial landmarks [33], [34], [35], [32], [36], latent representation [37] and so on. Cao *et al.* [38] utilized some RGBD sensors to create an extensive face database named FaceWareHouse, which contains 150 identities and 47 expressions of each identity. In recent years, deep learning-based methods have shown promising results in terms of computation time, robustness to occlusions and reconstruction accuracy. Guo *et al.* [39] proposed a real-time dense face reconstruction method by constructing a large scale dataset augmented based on traditional optimization methods and adopting a coarse-to-fine CNN framework. Gecer *et al.* [40] harnessed Generative Adversarial Networks (GANs) for reconstructing facial texture and shape from single images by training a generator of facial texture in UV space. Feng *et al.* [41] presented a model-free method to rebuild the 3D facial geometry from a single light field image with a densely connected network.

Face Alignment and Reconstruction of Caricature. Compared with researches on normal facial images, there are fewer works about caricatures [42], [43]. For face reconstruction, existing methods mainly focus on constructing a 3D caricature model from a normal 3D face model. Lewiner *et al.* [9] introduced a caricature tool that interactively emphasizes the differences between two 3D meshes by utilizing the manifold harmonic basis of a shape to control the deformation and scales intrinsically. Vieira *et al.* [10] proposed a method based on deformations by manipulation of moving spherical influence zones. Sela *et al.* [44] presented a framework to scale the gradient fields of the surface coordinates by a function of the Gaussian curvature of the surface and solve a corresponding Poisson equation to find the exaggerated shape. Besides, there are some works on modeling 3D caricatures from images. Liu *et al.* [45] chose a semi-supervised manifold regularization(MR) method to learn a regressive model between 2D normal faces and enlarged 3D caricatures. With the power of deep learning, Han *et al.* [11] developed a CNN based

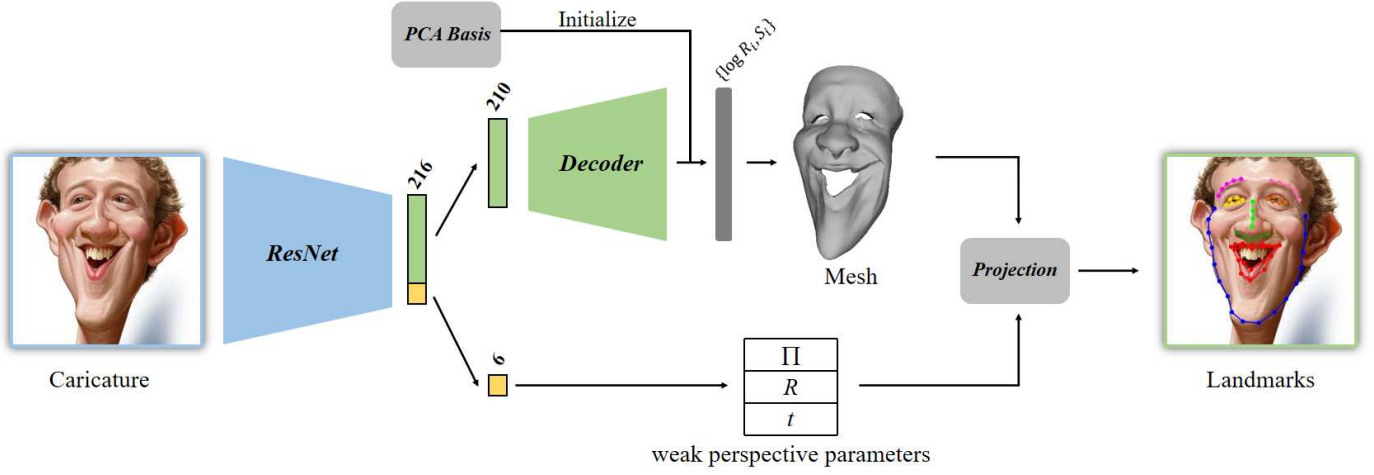


Fig. 2. Overview of our proposed Framework for Landmark Detection and 3D Reconstruction on general caricatures. Our network includes two parts, an encoder and a decoder. We use ResNet-34 [16] backbone as the encoder, and 3 Fully Connected(FC) layers as the decoder to recover the 3D caricature shape. The PCA basis of deformation presentation $\{\log \mathbf{R}_i, \mathbf{S}_i\}$ is used to initialize the last FC layer.

sketching system that allows users to draw freehand imprecise yet expressive 2D lines representing the contours of facial features. With an intrinsic deformation representation that enables considerable face exaggeration, Wu *et al.* [12] introduced an optimization framework to address this issue. We adopt this approach to construct the training set of 3D caricatures. Landmark detection on caricature images is also a fundamental problem of caricature perception, but there are few works on this topic. As a related research direction, manga images have aroused Stricker *et al.*'s [46] interest. Based on DAN [20] framework, they proposed a new landmark annotation model for manga images and a deep learning approach to detect them. Huo *et al.* [14] shows that caricature landmark detection is of great interest, but researches on this topic are still far from saturated. Besides, most studies on caricature generation need facial landmarks as control points [2], [4], [5], which demonstrate that facial landmarks play an essential role in caricature related researches.

III. ALGORITHM

Given a 2D caricature, we aim to automatically reconstruct its 3D face shape and obtain landmarks around its eyes, nose, mouth, and so on, as shown in Fig. 1. To this end, we construct a 2D caricature dataset, including manually labeled figures and machine-generated figures. We then build a 3D caricature dataset via an optimization method proposed in [12] with around 8K 2D caricatures and their corresponding labeled landmarks. In this way, we obtain its 3D shape and parameters of weak perspective projection for each caricature. Lastly, we propose a CNN-based algorithm to directly recover the 3D face shape parameters and orientation parameters from the input 2D caricature image. Notably, we use the principal component analysis (PCA) basis to initialize the weight of the last fully connected layer. The algorithm pipeline is shown in Fig. 2. In the following, we give the algorithm details for each component.

A. Dataset Construction and Augmentation

Currently, there exist some public available caricature datasets. For the study of caricature recognition, Huo *et al.* [14] constructed a WebCaricature database including 6042 caricatures and 5974 photographs from 252 persons with 17 labeled facial landmarks for each image. Mishra *et al.* [47] built IIIT-CFW database for face classification and caricature generation, which contains 8928 cartoon faces of 100 public figures with annotation of various attributes, e.g., face bounding box, age group, facial expression, and so on. However, these datasets can not be directly used for our task as they do not supply enough labeled landmarks for 3D reconstruction.

By searching and selecting nearly 6K various caricatures from different artists on the Internet, we construct a caricature dataset with 68 labeled landmarks. The landmark positions are initialized via the Dlib library [18], and then manually refined. To further increase the diversity of our dataset, we design a data augmentation method based on CariGANs [4]. It is able to translate normal facial images to caricatures with two generative adversarial networks (GANs), namely



Fig. 3. The first row shows some examples of our collected images with manually labeled landmarks, while the second row shows some examples of our augmented images and corresponding landmarks generated by [4].

CariGeoGAN and CariStyGAN. CariGeoGAN learns a mapping to exaggerate the shape by adjusting facial landmarks, while CariStyGAN learns another mapping to translate the appearance from normal facial image style to caricature style. With trained CariGANs, we can generate a caricature and its corresponding 68 landmarks from a given normal facial image. In this way, we generate around 2K caricatures and add them to our dataset. Some examples of our collected data and augmented data are shown in Fig. 3.

B. 3D Caricature Representation and Recovery

Parametric models such as 3DMM [15] are popularly used in 3D face reconstruction to represent complex face shapes with a low dimensional parametric vector. This kind of representation makes optimization and learning based 3D face reconstruction easier. However, linear parametric models are only good for *interpolation* in the shape space of normal 3D faces but do not work well for *extrapolation* in 3D caricature shape space. Therefore, to reconstruct 3D models from 2D caricatures, we adopt the deformation representation to recover 3D caricature shape, which is used in [12]. Compared with 3D Euclidean coordinates, this deformation representation is suitable to represent local and large deformation in a natural way, which makes the reconstructed exaggerated meshes more natural and match the input 2D caricature quite well.

To make our paper self-contained, we first introduce the deformation representation between two models with consistent connectivity and then give the algorithm details on how to recover the 3D caricature shape from the 2D landmarks. Firstly, we treat one model as a template and another as a target deformed model. We denote the position of the i^{th} vertex v_i on the template as \mathbf{p}_i and the i^{th} vertex v_i on the target as \mathbf{p}'_i . We can define the deformation gradient in the one-ring neighborhood of v_i from the template to the target as an affine transformation matrix \mathbf{T}_i by minimizing

$$\arg \min_{\mathbf{T}_i} \sum_{j \in \mathcal{N}_i} c_{ij} \|(\mathbf{p}'_i - \mathbf{p}'_j) - \mathbf{T}_i(\mathbf{p}_i - \mathbf{p}_j)\|_2^2, \quad (1)$$

where \mathcal{N}_i is the neighborhood index set of v_i , and c_{ij} is the cotangent weight [48] to avoid discretization bias in deformation. With polar decomposition, the deformation matrix \mathbf{T}_i can be decomposed into a rigid component represented by a rotation matrix \mathbf{R}_i and a non-rigid component represented by a real symmetry matrix \mathbf{S}_i , as $\mathbf{T}_i = \mathbf{R}_i \mathbf{S}_i$.

To obtain efficient linear combination, we use the axis-angle representation [49] to replace the rotation matrix \mathbf{R}_i . Following Rodrigues' rotation formula, for the i^{th} vertex v_i , we denote the cross-product matrix and rotation angle by \mathbf{K}_i , θ_i . We can convert \mathbf{R}_i to a matrix logarithm notation:

$$\log \mathbf{R}_i = \theta_i \mathbf{K}_i, \quad (2)$$

$$\mathbf{K}_i = \begin{bmatrix} 0 & -k_{i,z} & k_{i,y} \\ k_{i,z} & 0 & -k_{i,x} \\ -k_{i,y} & k_{i,x} & 0 \end{bmatrix}, \quad (3)$$

where $\mathbf{k}_i \in \mathbb{R}^3$ and $\|\mathbf{k}_i\|_2 = 1$. This representation has many advantages, especially for our method, it can be used

for linear combination [50] of two rotation matrices \mathbf{R}_i^0 and \mathbf{R}_i^1 by $\exp(\log \mathbf{R}_i^0 + \log \mathbf{R}_i^1)$. We choose a reference model and n deformed models which have the same connectivities with the reference model. For the i^{th} vertex of each deformed model, we obtain its deformation representation $\{\log \mathbf{R}_i^k, \mathbf{S}_i^k\} (k = 1, 2, \dots, n)$. Following [51], the logarithm rotation matrix can be represented by a vector $\mathbf{r}_i \in \mathbb{R}^3$ and the scalar matrix can be represented by a vector $\mathbf{s}_i \in \mathbb{R}^6$. To handle the ambiguity of axis-angle representation, Gao *et al.* [51] proposed an integer programming approach to make all \mathbf{r}_i as consistent as possible globally. Then, corresponding to an essential deformation representation, a target mesh can be approximately reconstructed by a linear combination of several known deformation gradients.

With the method of [12], we obtain the latent deformation representation for vertices' coordinates and the weak perspective parameters for each caricature. Based on a reference model and n deformed models, we propose a linear combination of deformation gradients for the i^{th} vertex as

$$\mathbf{T}_i(\mathbf{w}) = \exp\left(\sum_{k=1}^n w_{R,k} \log \mathbf{R}_i^k\right) \left(\mathbf{I} + \sum_{k=1}^n w_{S,k} (\mathbf{S}_i^k - \mathbf{I})\right), \quad (4)$$

where $\mathbf{w} = (\mathbf{w}_R, \mathbf{w}_S)$ is the combination weight vector, consisting of weights of rotation $\mathbf{w}_R = \{w_{R,k} | k = 1, \dots, n\}$ and weights of scaling/shear $\mathbf{w}_S = \{w_{S,k} | l = 1, \dots, n\}$.

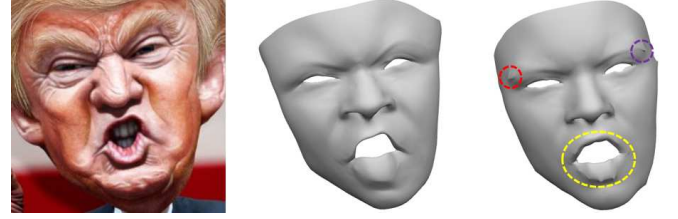


Fig. 4. Left to right: input caricature, 3D mesh reconstructed by our optimization model in Eq. (5), 3D mesh reconstructed by the optimization model in [12]. We can see that the result by [12] contains spikes around landmarks (highlighted with ellipses).

Given a caricature with labeled landmarks, we reconstruct the corresponding 3D caricature mesh by minimizing the following energy:

$$\begin{aligned} \min_{\mathbf{p}', \mathbf{w}, \mathbf{\Pi}, \mathbf{R}, \mathbf{t}} & \sum_{v_i \in \mathcal{V}} \sum_{j \in \mathcal{N}_i} c_{ij} \|(\mathbf{p}'_i - \mathbf{p}'_j) - \mathbf{T}_i(\mathbf{w})(\mathbf{p}_i - \mathbf{p}_j)\|_2^2 \\ & + \alpha_1 \sum_{v_i \in \mathcal{L}} \|\mathbf{\Pi} \mathbf{R} \mathbf{p}'_i + \mathbf{t} - \mathbf{q}_i\|^2 \\ & + \alpha_2 \sum_{v_i \in \mathcal{L}} \left\| \sum_{j \in \mathcal{N}_i} c_{ij} (\mathbf{p}'_i - \mathbf{p}'_j) - \sum_{j \in \mathcal{N}_i} c_{ij} (\mathbf{p}_i - \mathbf{p}_j) \right\|^2, \end{aligned} \quad (5)$$

where \mathcal{L} and $\mathcal{Q} = \{\mathbf{q}_i, v_i \in \mathcal{L}\}$ are the set of 3D landmarks and 2D landmarks separately, $\mathbf{\Pi}$ is the scaled projection matrix, \mathbf{R} is the rotation matrix constructed from Euler angles *pitch*, *yaw*, *roll* and $\mathbf{t} = [t_x, t_y]^T$ is the translation vector. The third term of Eq. (5) is the Laplacian smoothing term [?], and c_{ij} is the cotangent Laplacian weight of the neutral face mesh. The hyperparameters λ_1 and λ_2 are set as $\alpha_1 = 0.01$, $\alpha_2 = 1$. Note that, the optimization formulation in [12] does

not include the third term, and it will cause spikes around the landmarks, as shown in Fig. 4. An alternative optimization strategy is applied to solve the problem in Eq. (5) by fixing one set of variables while optimizing another set of variables, and alternating this process. After optimization, we can obtain the 3D coordinates \mathbf{P}' of target caricature mesh, weak perspective parameters, face orientation, and the combination parameters $\mathbf{w} = (\mathbf{w}_R, \mathbf{w}_S)$.

As the deformation representation for each vertex contains 9 variables, the deformation representation of the 3D caricature model with n_v vertices can be represented as a $9n_v$ vector. Therefore, given a 2D caricature, training a CNN model that ends with several fully connected layers to directly regress its corresponding $9n_v$ deformation representation vector is quite natural.



Fig. 5. First row: Input 2D caricatures. Second row: 3D models generated by [12]. Third row: 3D models recovered by the linear combination coefficients $\mathbf{w} = (\mathbf{w}_R, \mathbf{w}_S)$ of latent deformation representation as the result of [12]. Fourth row: 3D models generated by our algorithm.

C. Landmark Detection and Reconstruction

Although we adopt the deformation representation to recover the 3D caricature shape from the 2D image, the shape recovered only by $\mathbf{T}_i(\mathbf{w})$ can not represent the exaggerated part. Specifically, we can obtain the optimal linear combination coefficients $\mathbf{w} = (\mathbf{w}_R, \mathbf{w}_S)$ of latent deformation representation by solving Eq. (5) and recover a 3D shape from \mathbf{w} via Eq. (4). However, this shape can not match the ground truth caricature shapes, as shown in the third row of Fig. 5. This is because their methods are based on FaceWareHouse, a real face database. The reason why their final face shapes in [12] match the caricature shapes quite well is that the shape is further deformed based on the 2D landmarks, as the

second term in Eq. (5). Therefore, directly regressing the \mathbf{w} parameters can not satisfy our needs.

To solve this problem, we propose a CNN-based approach to directly regress the intrinsic deformation representation and the weak perspective projection parameters with a single 2D caricature image. As shown in Fig. 2, we utilize ResNet-34 backbone [16] to encode the input 2D caricature into a latent vector $\chi \in \mathbb{R}^{216}$. The latent vector contains two parts, where $\chi_s \in \mathbb{R}^{210}$ represents the 3D shape and $\chi_p \in \mathbb{R}^6$ represents the parameters of weak perspective projection. We propose a decoder composed of 3 fully connected layers to convert χ_s to the estimated latent deformation representation $\{[\hat{\mathbf{r}}_i, \hat{\mathbf{s}}_i], i = 1, \dots, n_v\}$, where n_v is the number of mesh vertices. The deformation gradients $\{(\log \hat{\mathbf{R}}_i, \hat{\mathbf{S}}_i), i = 1, \dots, n_v\}$ and $\hat{\mathbf{T}}_i$ then can be recovered accordingly. To help the model training, we initialize the weights of the last fully connected (FC) layer by a PCA basis extracted from the training dataset. The first 500 principal components are used to initialize the weights of the last FC layer.

Loss for Caricature Shape. As before, the estimated vertex coordinate $\{\hat{\mathbf{p}}'_i\}$ of target mesh can be obtained by solving

$$\arg \min_{\{\hat{\mathbf{p}}'_i\}} \sum_{j \in \mathcal{N}_i} c_{ij} \|(\hat{\mathbf{p}}'_i - \hat{\mathbf{p}}'_j) - \hat{\mathbf{T}}_i(\mathbf{p}_i - \mathbf{p}_j)\|_2^2, \quad (6)$$

which is equivalent to solve the following linear system:

$$2 \sum_{j \in \mathcal{N}_i} c_{ij} (\hat{\mathbf{p}}'_i - \hat{\mathbf{p}}'_j) = \sum_{j \in \mathcal{N}_i} c_{ij} (\hat{\mathbf{T}}_i + \hat{\mathbf{T}}_j)(\mathbf{p}_i - \mathbf{p}_j). \quad (7)$$

As the deformation representation is translation independent, and thus we need to specify the position of mesh center or exactly one vertex. As the ground truth 3D caricature meshes are under the same specification, we construct a loss term to constrain the coordinate difference between the reconstructed mesh and the ground truth mesh as

$$\mathbf{E}_{ver}(\chi_s) = \sum_{v_i \in \mathcal{V}} \|\hat{\mathbf{p}}'_i - \mathbf{p}'_i\|_2^2, \quad (8)$$

where \mathbf{p}'_i presents the ground truth coordinate of the i^{th} vertex of 3D mesh, and \mathcal{V} represents the vertex set.

Loss for Landmarks. Reconstructing the 3D mesh from a 2D image is the inverse process of observing a 3D object by projecting it to 2D visual space. As before, we assume that the projection plane is the z -plane and thus the scaled projection matrix can be written as $\mathbf{\Pi} = s \begin{bmatrix} 1 & 0 & 0 \\ 0 & 1 & 0 \end{bmatrix}$, where s is the scale factor. To better recover the landmark positions, we construct a landmark loss term to measure the difference between the projected landmarks and the ground truth landmarks:

$$\mathbf{E}_{lan}(\chi) = \sum_{v_i \in \mathcal{L}'} \|\hat{\mathbf{\Pi}} \hat{\mathbf{R}} \hat{\mathbf{p}}'_i + \hat{\mathbf{t}} - \mathbf{q}'_i\|_2^2, \quad (9)$$

where \mathcal{L}' and $\mathcal{Q}' = \{\mathbf{q}'_i, v_i \in \mathcal{L}'\}$ are the set of 3D landmarks and 2D landmarks separately, $\hat{\mathbf{\Pi}}$ is the estimated scaled projection matrix, $\hat{\mathbf{R}}$ is the estimated rotation matrix, and $\hat{\mathbf{t}}$ is

the estimated translation vector. As our 3D caricature meshes have the same connectivities, the indices of 3D landmarks are the same for different caricature shapes.

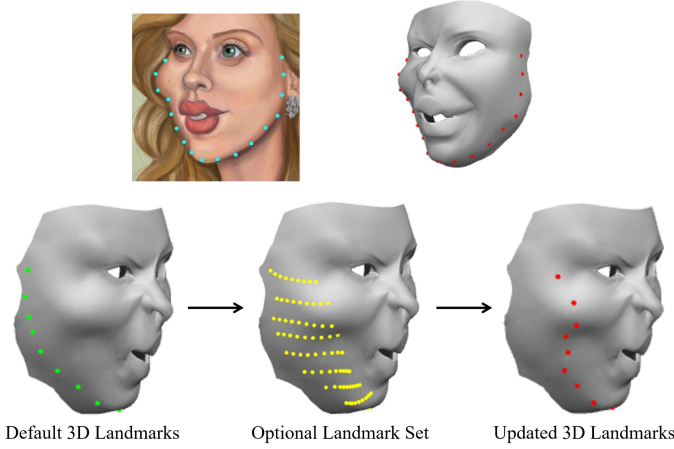


Fig. 6. For non-frontal face caricatures, we need to update the indices of silhouette landmarks on the 3D face shape to better match the corresponding 2D landmarks (shown in cyan in upper-left). The default 3D silhouette landmarks are shown in green in the lower-left. We construct an optional landmark set from each horizontal line (shown in yellow in lower-middle) that has a vertex lying on the silhouette and select among them a set of the updated silhouette landmarks according to the estimated rotation matrix $\hat{\mathbf{R}}$ in each training time. The vertices of the silhouette are updated in the end as shown in red on the upper right and lower-right.

Compared with normal face, the positions of caricature silhouette landmarks have large variance, and thus it is quite challenging to detect their positions accurately. Moreover, the 3D vertices corresponding with these silhouette landmarks are labeled on the mean neutral face with a frontal view, which causes the problem that the correspondences between 3D vertices and 2D landmarks are not correct for non-frontal faces as shown in Fig. 6. To solve this problem, we update the indices of 3D silhouette landmarks each training time according to the estimated rotation matrix and vertices' coordinates. In each time, we select some vertices from each horizontal line that has a vertex lying on the silhouette and project them onto the image plane according to the estimated rotation matrix $\hat{\mathbf{R}}$. Then for each 2D silhouette landmark, we set the vertex whose projection is closest to it (see Fig. 6) as its current corresponding 3D silhouette landmark.

Loss for Projection Parameters. To recover the 2D landmarks from the 3D shape, we also need to regress the parameters of weak perspective projection for each caricature. We find that the MSE between predicted parameters and ground truth parameters can not generate a good result. A better way is to constrain the projection difference between the ground truth 3D landmark with ground truth projection parameters $(\mathbf{s}, \mathbf{R}, \mathbf{t})$ and estimated parameters $(\hat{\mathbf{s}}, \hat{\mathbf{R}}, \hat{\mathbf{t}})$:

$$\mathbf{E}_{srt}(\chi_p) = \sum_{v_i \in \mathcal{L}'} \|(\hat{\mathbf{R}}\mathbf{p}'_i + \hat{\mathbf{t}}) - (\mathbf{R}\mathbf{p}'_i + \mathbf{t})\|_2^2, \quad (10)$$

where \mathbf{p}'_i represents the ground truth 3D landmark position.

The total loss function is given in the following form:

$$\mathbf{E} = \lambda_1 \mathbf{E}_{ver} + \lambda_2 \mathbf{E}_{lan} + \lambda_3 \mathbf{E}_{srt}, \quad (11)$$

where $\lambda_1, \lambda_2, \lambda_3$ are hyperparameters and their setting will be discussed in the experiment section.

IV. EXPERIMENTS

In this section, we conduct qualitative and quantitative evaluation of our proposed landmark detection and 3D reconstruction method for caricature and compare it with several baseline methods.

Implementation Details We train our model via the PyTorch [52] framework. CNN takes the input of a color caricature image with size $224 \times 224 \times 3$. We use Adam solver [53] with the mini-batch size of 32 and train the model with 2K iterations. The base learning rate is set to 0.0001. We set $\lambda_1 = 1, \lambda_2 = 0.00001, \lambda_3 = 0.00001$ during the first 1K iterations, and set $\lambda_1 = 1, \lambda_2 = 0.001, \lambda_3 = 0.00001$ during the last 1K iterations. The reason why the magnitudes of parameters are quite different is that the magnitude of vertices' coordinates has a big difference with that of 2D pixels.

All the tests, including our method, baseline methods and comparison methods, were conducted on a desktop PC with a hexa-core Intel CPU i7 at 3.40 GHz, 16GB of RAM and NVIDIA TITAN Xp GPU. As for the running time for each caricature, our method takes about 10ms to obtain both 3D mesh and 68 2D landmarks. The number of vertices of our reconstructed mesh is 6144.

A. Landmark Detection Comparison

As far as we know, there is no existing method for landmark detection for general caricatures. We compare our method with some baseline methods. The first type is the face alignment methods, which are designed for normal human faces, and we select three typical methods, including DAN [20], ERT [17], and vanilla CNN (VCNN) designed by [19]. As their released trained models are trained with normal facial images, we retrain their models based on the author's training code. For a fair comparison, their methods are trained and tested with the same training and testing dataset as our method. We randomly split our dataset into 80% for training and 20% for testing.

DAN: Deep Alignment Network (DAN) [20] is a robust face alignment method based on deep neural network architecture. Its algorithm pipeline includes multiple stages, where each stage improves the locations of the facial landmarks estimated by the previous stage.

ERT: In [17], an ensemble of regression trees (ERT) has been used to directly estimate the facial landmark positions from a sparse subset of pixel intensities. This method achieves super-realtime performance with high-quality predictions. It has been integrated into Dlib library [18].

VCNN: Vanilla CNN is proposed in [19], which introduces hierarchical and discriminative processing to existing CNN design for facial landmark regression.

L-PCA: Except for the above three methods, we also implement some baseline methods. Inspired by [4], we extract the PCA basis of 2D caricature landmarks from the labeled landmark dataset. In this way, the landmarks of caricature image can be represented by the coefficient of PCA basis.



Fig. 7. We provide visual landmark detection results on the test dataset using DAN [20], ERT [17], VCN [19] and some baselines including Landmark PCA (L-PCA), Vertex PCA (V-PCA), and DR-PCA.

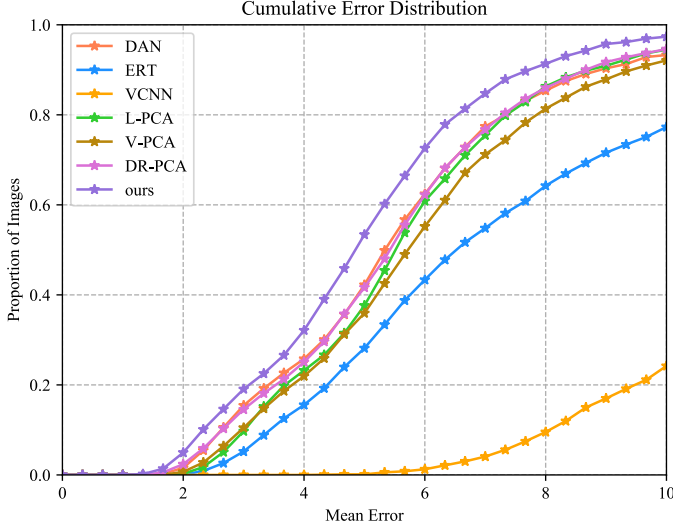


Fig. 8. Comparisons of cumulative errors distribution (CED) curves on the test set.

We use the same ResNet framework in our method to directly regress the coefficient.

V-PCA: We extract the PCA basis of 3D caricature shape set represented by the Euclidean coordinates. The network structure is the same with our algorithm pipeline in Fig. 2,

TABLE I
STATISTICS OF LANDMARK DETECTION ERRORS AND COMPUTATION TIME (MS/IMAGE) ON THE TEST SET. VALUES OF MEAN ERROR WITH NORMALIZATION ARE SHOWN AS THE PERCENTAGE OF THE NORMALIZATION METRIC.

	mean error	inter-pupil	inter-ocular	diagonal	time (ms)
DAN	5.78	9.93	6.80	2.59	25.9
ERT	8.24	14.52	9.95	3.71	2.7
VCNN	14.04	24.33	16.67	6.39	1.6
L-PCA	5.87	10.08	6.91	2.64	5.0
V-PCA	6.20	10.68	7.32	2.79	6.7
DR-PCA	5.75	9.89	6.77	2.58	10.0
Ours	5.06	8.60	5.89	2.27	10.5

and regresses the PCA coefficient and orientation.

DR-PCA: We extract the PCA basis of 3D caricature shape set represented by the deformation representation. The pipeline is the same as ours by replacing the decoder part with the extracted PCA basis.

We compare our method with state-of-the-art methods and baselines. Fig. 7 shows some visual results of landmark detection. It can be observed that the detected landmarks of ERT [17] and VCN [19] can not match the face shape. The method of DAN [20] performs quite well for the facial feature parts, including eyes, nose and mouth. However, its silhouette landmarks may deviate from the accurate positions.

V-PCA and L-PCA are also not good for the landmarks on the silhouette. Though DR-PCA representation shows nice performance, it still can not match the facial feature parts precisely. In contrast, the detection results by our method are quite close to the ground truth landmarks, even for the silhouette landmarks. We also quantitatively compare our method with these methods on several frequently used landmark error metrics and average computation time. We show the statistics in Tab. I and the cumulative errors distribution (CED) curves of these methods on the mean error in Fig. 8. We can see that the mean error, mean error normalized separately by inter-pupil distance, inter-ocular distance and bounding box diagonal of our methods are all smaller than those of other methods.

The reason why our method performs better includes the following aspects. First, rather than directly regressing the 2D landmarks, we regress the 3D shape and orientation. In this way, a hard problem is decomposed into two easier problems. Second, to better represent the 3D caricature shape, we learn a nonlinear parametric model, which is more suitable to represent the 3D caricature shape than 3D morphable model [15] and FaceWareHouse [38].



Fig. 9. Left to right: input caricature, predicted mesh overlaying on the image, predicted mesh in two different views, predicted mesh with texture.

B. 3D Reconstruction Comparison

Reconstructing 3D caricature shape from caricature image is also a challenging problem, and the only related work is [12]. We adopt the method of [12] to construct the 3D caricature dataset. As shown in their paper, parametric models like 3DMM [54], [55] and FaceWareHouse [38] cannot reconstruct exaggerated meshes well due to their limited extrapolation ability. The algorithm of [12] is given in Sec. III-B, and we compare our 3D reconstruction results with this method.

In Fig. 9, we show two reconstruction examples from the test set. The reconstructed mesh is overlaid on the image, and we can observe that the shape is recovered quite well. The recovered mesh from two different views and with texture are also shown to demonstrate the effectiveness of our method. Furthermore, from Fig. 10, we can find that the reconstructed 3D meshes by our method are quite close to the results by [12]. As their results supervise the ground truth meshes during training, it demonstrates the nice performance of our trained model to fit the ground truth 3D shapes. One advantage of our method over [12] is the computation time. It takes around 10ms to produce the result with our method, while 12.5s for their method. Moreover, our reconstruction method does not need to label the landmarks manually.

From the above quantitative and qualitative experiments, we can see that our proposed method performs quite well on landmark detection and reconstruction for caricatures and non-caricature faces with exaggerated expressions. In Fig. 11 and Fig. 12, more experimental results and comparisons with the state-of-the-art landmark detection methods [20], [17], [19] and 3D caricature reconstruction method [12] on 20 test caricatures are given. These results further validate the superior effect of our proposed method on the tasks of landmark detection and 3D reconstruction on caricature.

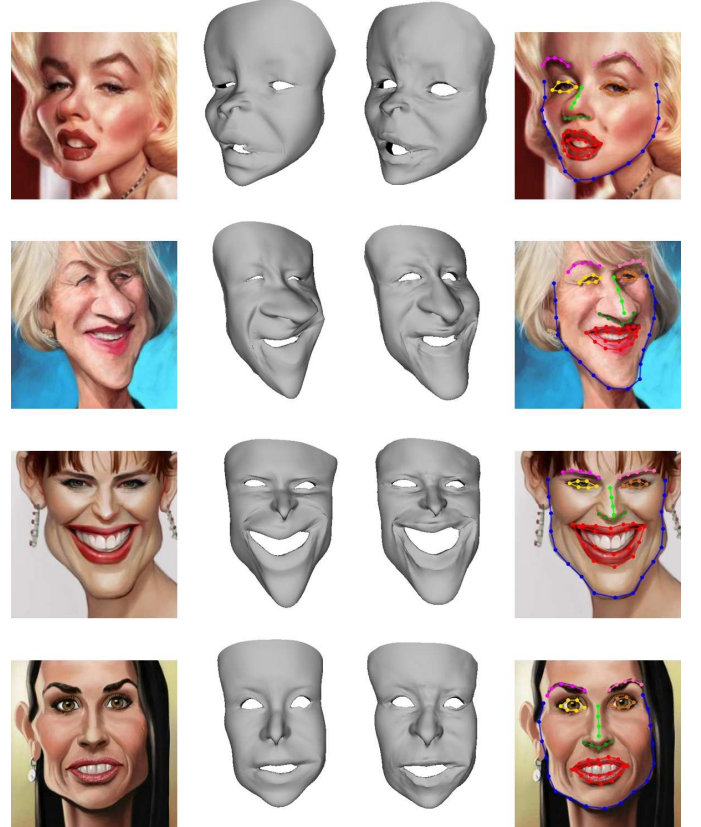


Fig. 10. Reconstruction results by our method and [12]. From the first column to the last column are input images, reconstruction results by [12], reconstruction results by our method, and the projected 2D landmarks by our method respectively.

V. CONCLUSION

We have presented an effective and efficient algorithm for automatic landmark detection and 3D reconstruction for 2D caricature images. This challenging problem is well solved by separately regressing the 3D face shape and face pose, and then 2D landmarks and 3D shape can both be obtained. To represent the non-regular 3D caricature face, we construct a 3D caricature shape dataset to learn the latent representation. Extensive experimental results show that the detected 2D landmarks and reconstructed 3D face shape fit the caricature quite well, which outperforms the state-of-the-art methods in both computation speed and accuracy.

Acknowledgement This work was supported by the National Natural Science Foundation of China (No. 61672481) and Youth Innovation Promotion Association CAS (No. 2018495).



Fig. 11. Landmark detection comparisons with state-of-art methods DAN [20], ERT [17], VCNN [19] and reconstruction comparisons with Alive [12] which needs labeled landmarks. It can be seen that our method can detect landmarks and reconstruct 3D face shapes quite well.



REFERENCES

- [1] S. E. Brennan, "Caricature generator: The dynamic exaggeration of faces by computer," *Leonardo*, vol. 18, no. 3, pp. 170–178, 1985.
- [2] L. Liang, H. Chen, Y. Xu, and H. Shum, "Example-based caricature generation with exaggeration," in *10th Pacific Conference on Computer Graphics and Applications*, 2002, pp. 386–393.
- [3] H.-Y. Shum, Y.-Q. Xu, M. F. Cohen, and H. Zhong, "Sample based face caricature generation."
- [4] K. Cao, J. Liao, and L. Yuan, "Carigans: unpaired photo-to-caricature translation," *ACM Transactions on graphics (TOG)*, vol. 37, no. 6, pp. 244:1–244:14, 2018.
- [5] Y. Shi, D. Deb, and A. K. Jain, "WarpGAN: Automatic caricature generation," in *IEEE Conference on Computer Vision and Pattern Recognition (CVPR)*, 2019, pp. 10762–10771.
- [6] B. Klare, S. S. Bucak, A. K. Jain, and T. Akgul, "Towards automated caricature recognition," in *5th IAPR International Conference on Biometrics, ICB*, 2012, pp. 139–146.
- [7] S. Ouyang, T. M. Hospedales, Y. Song, and X. Li, "Cross-modal face matching: Beyond viewed sketches," in *12th Asian Conference on Computer Vision*, 2014, pp. 210–225.
- [8] B. Abaci and T. Akgul, "Matching caricatures to photographs," *Signal, Image and Video Processing*, vol. 9, no. Supplement-1, pp. 295–303, 2015.
- [9] T. Lewiner, T. Vieira, D. Martínez, A. Peixoto, V. Mello, and L. Velho, "Interactive 3d caricature from harmonic exaggeration," *Computers & Graphics*, vol. 35, no. 3, pp. 586–595, 2011.
- [10] R. C. C. Vieira, C. A. Vidal, and J. B. C. Neto, "Three-dimensional face caricaturing by anthropometric distortions," in *XXVI Conference on Graphics, Patterns and Images, SIBGRAPI*, 2013, pp. 163–170.
- [11] X. Han, C. Gao, and Y. Yu, "DeepSketch2face: a deep learning based sketching system for 3d face and caricature modeling," *ACM Transactions on graphics (TOG)*, vol. 36, no. 4, pp. 126:1–126:12, 2017.
- [12] Q. Wu, J. Zhang, Y.-K. Lai, J. Zheng, and J. Cai, "Alive caricature from 2d to 3d," in *IEEE Conference on Computer Vision and Pattern Recognition (CVPR)*, 2018, pp. 7336–7345.
- [13] S. Sadimon and H. Haron, "Neural network model for prediction of facial caricature landmark configuration using modified procrustes superimposition method," *International Journal of Advances in Soft Computing & Its Applications*, vol. 7, no. 3, 2015.
- [14] J. Huo, W. Li, Y. Shi, Y. Gao, and H. Yin, "Webcaricature: a benchmark for caricature recognition," in *British Machine Vision Conference (BMVC)*, 2018, p. 223.
- [15] V. Blanz, T. Vetter *et al.*, "A morphable model for the synthesis of 3d faces," in *Siggraph*, vol. 99, no. 1999, 1999, pp. 187–194.
- [16] K. He, X. Zhang, S. Ren, and J. Sun, "Deep residual learning for image recognition," in *IEEE Conference on Computer Vision and Pattern Recognition (CVPR)*, 2016, pp. 770–778.
- [17] V. Kazemi and J. Sullivan, "One millisecond face alignment with an ensemble of regression trees," in *IEEE Conference on Computer Vision and Pattern Recognition (CVPR)*, 2014, pp. 1867–1874.
- [18] D. E. King, "Dlib-ml: A machine learning toolkit," *Journal of Machine Learning Research*, vol. 10, pp. 1755–1758, 2009.
- [19] Y. Wu, T. Hassner, K. Kim, G. G. Medioni, and P. Natarajan, "Facial landmark detection with tweaked convolutional neural networks," *IEEE Transactions on Pattern Analysis and Machine Intelligence*, vol. 40, no. 12, pp. 3067–3074, 2018.
- [20] M. Kowalski, J. Naruniec, and T. Trzcinski, "Deep alignment network: A convolutional neural network for robust face alignment," in *IEEE Conference on Computer Vision and Pattern Recognition Workshops, CVPR Workshops*, 2017, pp. 2034–2043.
- [21] R. Valle, J. M. Buenaposada, A. Valdés, and L. Baumela, "A deeply-initialized coarse-to-fine ensemble of regression trees for face alignment," in *European Conference on Computer Vision (ECCV)*, 2018, pp. 585–601.
- [22] Z. Liu, X. Zhu, G. Hu, H. Guo, M. Tang, Z. Lei, N. M. Robertson, and J. Wang, "Semantic alignment: Finding semantically consistent ground-truth for facial landmark detection," in *IEEE Conference on Computer Vision and Pattern Recognition (CVPR)*, 2019, pp. 3467–3476.
- [23] X. Dong, S.-I. Yu, X. Weng, S.-E. Wei, Y. Yang, and Y. Sheikh, "Supervision-by-registration: An unsupervised approach to improve the precision of facial landmark detectors," in *IEEE Conference on Computer Vision and Pattern Recognition (CVPR)*, 2018, pp. 360–368.
- [24] S. Honari, P. Molchanov, S. Tyree, P. Vincent, C. Pal, and J. Kautz, "Improving landmark localization with semi-supervised learning," in *IEEE Conference on Computer Vision and Pattern Recognition (CVPR)*, 2018, pp. 1546–1555.
- [25] M. Zhu, D. Shi, M. Zheng, and M. Sadiq, "Robust facial landmark detection via occlusion-adaptive deep networks," in *IEEE Conference on Computer Vision and Pattern Recognition (CVPR)*, 2019, pp. 3486–3496.
- [26] D. Merget, M. Rock, and G. Rigoll, "Robust facial landmark detection via a fully-convolutional local-global context network," in *IEEE conference on computer vision and pattern recognition (CVPR)*, 2018, pp. 781–790.
- [27] V. Blanz and T. Vetter, "Face recognition based on fitting a 3d morphable model," *IEEE Transactions on pattern analysis and machine intelligence*, vol. 25, no. 9, pp. 1063–1074, 2003.
- [28] A. Tuan Tran, T. Hassner, I. Masi, and G. Medioni, "Regressing robust and discriminative 3d morphable models with a very deep neural network," in *Proceedings of the IEEE Conference on Computer Vision and Pattern Recognition*, 2017, pp. 5163–5172.
- [29] X. Zhu, Z. Lei, X. Liu, H. Shi, and S. Z. Li, "Face alignment across large poses: A 3d solution," in *IEEE Conference on Computer Vision and Pattern Recognition (CVPR)*, 2016, pp. 146–155.
- [30] Y. Feng, F. Wu, X. Shao, Y. Wang, and X. Zhou, "Joint 3d face reconstruction and dense alignment with position map regression network," in *European Conference on Computer Vision (ECCV)*, 2018, pp. 534–551.
- [31] J. Thies, M. Zollhöfer, M. Nießner, L. Valgaerts, M. Stamminger, and C. Theobalt, "Real-time expression transfer for facial reenactment," *ACM Transactions on Graphics (TOG)*, vol. 34, no. 6, pp. 183:1–183:14, 2015.
- [32] J. Thies, M. Zollhofer, M. Stamminger, C. Theobalt, and M. Nießner, "Face2face: Real-time face capture and reenactment of rgb videos," in *IEEE Conference on Computer Vision and Pattern Recognition (CVPR)*, 2016, pp. 2387–2395.
- [33] C. Cao, Q. Hou, and K. Zhou, "Displaced dynamic expression regression for real-time facial tracking and animation," *ACM Transactions on graphics (TOG)*, vol. 33, no. 4, p. 43, 2014.
- [34] L. A. Jeni, J. F. Cohn, and T. Kanade, "Dense 3d face alignment from 2d videos in real-time," in *IEEE international conference and workshops on automatic face and gesture recognition (FG)*, vol. 1. IEEE, 2015, pp. 1–8.
- [35] C. M. Grewe and S. Zachow, "Fully automated and highly accurate dense correspondence for facial surfaces," in *European Conference on Computer Vision (ECCV)*. Springer, 2016, pp. 552–568.
- [36] L. Jiang, J. Zhang, B. Deng, H. Li, and L. Liu, "3d face reconstruction with geometry details from a single image," *IEEE Transactions on Image Processing*, vol. 27, no. 10, pp. 4756–4770, 2018.
- [37] P. Huber, Z.-H. Feng, W. Christmas, J. Kittler, and M. Ratsch, "Fitting 3d morphable face models using local features," in *IEEE international conference on image processing (ICIP)*. IEEE, 2015, pp. 1195–1199.
- [38] C. Cao, Y. Weng, S. Zhou, Y. Tong, and K. Zhou, "Facewarehouse: A 3d facial expression database for visual computing," *IEEE Transactions on Visualization and Computer Graphics*, vol. 20, no. 3, pp. 413–425, 2013.
- [39] Y. Guo, J. Zhang, J. Cai, B. Jiang, and J. Zheng, "Cnn-based real-time dense face reconstruction with inverse-rendered photo-realistic face images," *IEEE Transactions on Pattern Analysis and Machine Intelligence*, vol. 41, no. 6, pp. 1294–1307, 2019.
- [40] B. Gecer, S. Ploumpis, I. Kotsia, and S. Zafeiriou, "Ganfit: Generative adversarial network fitting for high fidelity 3d face reconstruction," in *IEEE Conference on Computer Vision and Pattern Recognition (CVPR)*, 2019, pp. 1155–1164.
- [41] M. Feng, S. Zulqarnain Gilani, Y. Wang, and A. Mian, "3d face reconstruction from light field images: A model-free approach," in *European Conference on Computer Vision (ECCV)*, 2018, pp. 501–518.
- [42] A. J. O'toole, T. Vetter, H. Volz, and E. M. Salter, "Three-dimensional caricatures of human heads: distinctiveness and the perception of facial age," *Perception*, vol. 26, no. 6, pp. 719–732, 1997.
- [43] A. J. O'Toole, T. Price, T. Vetter, J. C. Bartlett, and V. Blanz, "3d shape and 2d surface textures of human faces: The role of averages in attractiveness and age," *Image and Vision Computing*, vol. 18, no. 1, pp. 9–19, 1999.
- [44] M. Sela, Y. Aflalo, and R. Kimmel, "Computational caricaturization of surfaces," *Computer Vision and Image Understanding*, vol. 141, pp. 1–17, 2015.
- [45] J. Liu, Y. Chen, C. Miao, J. Xie, C. X. Ling, X. Gao, and W. Gao, "Semi-supervised learning in reconstructed manifold space for 3d caricature generation," in *Computer Graphics Forum*, vol. 28, no. 8. Wiley Online Library, 2009, pp. 2104–2116.
- [46] M. Stricker, O. Augereau, K. Kise, and M. Iwata, "Facial landmark detection for manga images," *CoRR*, vol. abs/1811.03214, 2018.

- [47] A. Mishra, S. N. Rai, A. Mishra, and C. V. Jawahar, "IIIT-CFW: A benchmark database of cartoon faces in the wild," in *Computer Vision - ECCV Workshops*, 2016, pp. 35–47.
- [48] M. Botsch and O. Sorkine, "On linear variational surface deformation methods," *IEEE Transactions on Visualization and Computer Graphics*, vol. 14, no. 1, pp. 213–230, 2007.
- [49] J. Diebel, "Representing attitude: Euler angles, unit quaternions, and rotation vectors," *Matrix*, vol. 58, no. 15-16, pp. 1–35, 2006.
- [50] M. Alexa, "Linear combination of transformations," in *ACM Transactions on Graphics (TOG)*, vol. 21, no. 3. ACM, 2002, pp. 380–387.
- [51] L. Gao, Y. Lai, J. Yang, L. Zhang, L. Kobbelt, and S. Xia, "Sparse data driven mesh deformation," *CoRR*, vol. abs/1709.01250, 2017.
- [52] A. Paszke, S. Gross, S. Chintala, G. Chanan, E. Yang, Z. DeVito, Z. Lin, A. Desmaison, L. Antiga, and A. Lerer, "Automatic differentiation in PyTorch," in *NIPS Autodiff Workshop*, 2017.
- [53] D. P. Kingma and J. Ba, "Adam: A method for stochastic optimization," in *International Conference on Learning Representations (ICLR)*, 2015.
- [54] P. Paysan, R. Knothe, B. Amberg, S. Romdhani, and T. Vetter, "A 3d face model for pose and illumination invariant face recognition," in *Sixth IEEE International Conference on Advanced Video and Signal Based Surveillance, AVSS 2009, 2-4 September 2009, Genova, Italy*, 2009, pp. 296–301.
- [55] X. Zhu, Z. Lei, J. Yan, D. Yi, and S. Z. Li, "High-fidelity pose and expression normalization for face recognition in the wild," in *IEEE Conference on Computer Vision and Pattern Recognition, CVPR 2015, Boston, MA, USA, June 7-12, 2015*, 2015, pp. 787–796.